

# Discrepancies in Shortwave Diffuse Measured and Modeled Irradiances in Antarctica

*A. Payton, P. Ricchiazzi, and C. Gautier*  
*University of California*  
*Santa Barbara, California*

*D. Lubin*  
*Scripps*  
*Scripps Institution of Oceanography*  
*La Jolla, California*

## Introduction

Measurements of clear-sky shortwave (SW) radiation at the surface show discrepancies between measurements and model simulations, but only for certain measurements across time and space. Most of the observations entail broadband measurements. A spectral and spatial analysis of the occurrence of this discrepancy may lend insight into the responsible processes. Langley calibrated multi-filter rotating shadowband radiometer (MFRSR) measurements collected at the Antarctic coastline reveal significant discrepancies in modeled versus measured diffuse irradiance. Measurements were made over the 1999 to 2000 summer season at Palmer Station, a low-altitude U.S. research station off the Antarctic Peninsula. The standard error ( $2\sigma$ ) of the calibration is within 2% for all MFRSR channels and a Monte Carlo model, Surface-Atmosphere Monte Carlo Radiative Transfer (SAMCRT), is used to explicitly simulate surface condition around the measurement site for all calculations. Three clear-sky days show low aerosol optical depth and diffuse irradiances that are below modeled values and exhibit strong wavelength dependence. Careful examination of instrument calibration, optical depth retrievals, and models inputs suggest that this discrepancy is not due to measurement or modeling error.

## Analysis

The MFRSR data was calibrated in situ using Langley regressions collected in Santa Barbara, California over a 13 month period encompassing the Antarctic field season. The spectral calibration has a standard error ( $2\sigma$ ) of less than 2% for all channels and systematic bias representing sensor degradation through time that is accounted for in the calibration of the data. Figure 1 shows the zero air mass intercepts for the five MFRSR channels used in the analysis: 415 nm, 500 nm, 615 nm, 670 nm, and 870 nm. The linear regression fit represents sensor drift through time which is accounted for in the calibration of the data. Angular calibrations were also performed before and after the field season in March 1999 and June 2000 and show little change in the cosine response over time. The response is normalized to the ideal cosine response. Table 1 gives the mean, standard deviation, and standard error of the 72 Langley events. The two standard deviation standard error estimate is less than 2% for all five channels.

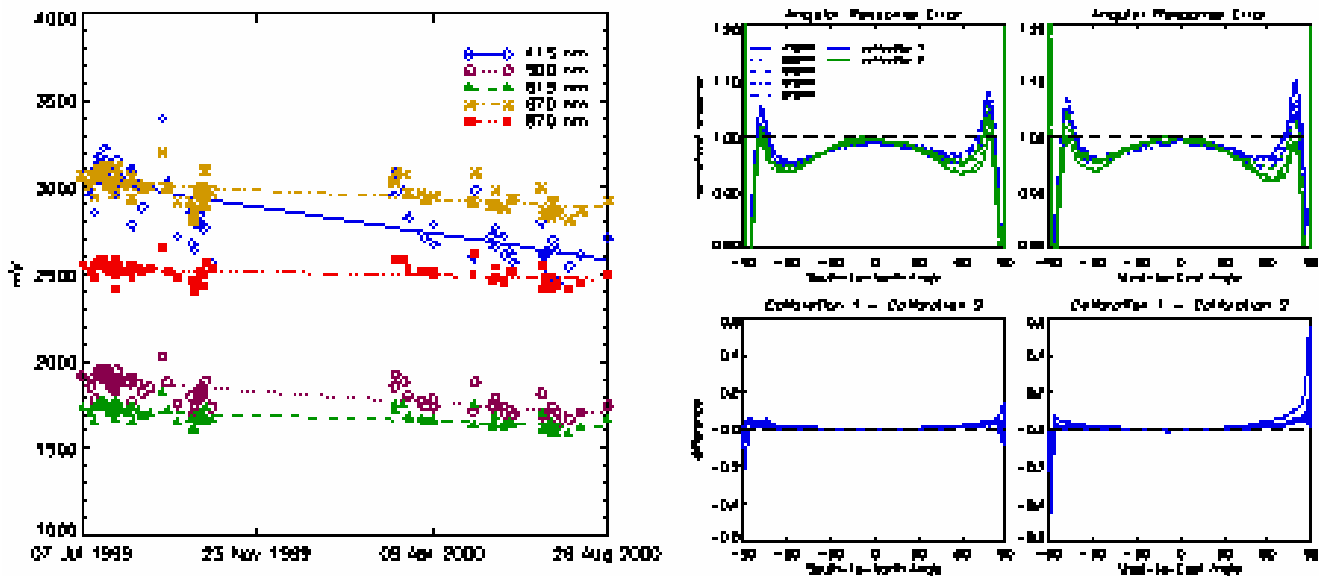


**Figure 1.** Zero airmass intercepts from Langley analysis of 72 events occurring in Santa Barbara, California for the five MFRSR channels and cosine response functions for two calibrations.

<b>Table 1.</b> Standard error estimation of in situ calibration for the 72 Langley events at the 95% confidence interval level.					
N = 72	415 nm	500 nm	615 nm	670 nm	870 nm
Mean	2861.0	1813.9	1686.0	2977.0	2512.5
Standard Deviation	214.49	90.37	55.46	86.95	54.09
% Standard Deviation	7.5%	5.0%	3.3%	2.9%	2.2%
Standard Error ( $2\sigma$ )	49.54	20.87	12.81	20.08	12.50
% Standard Error ( $2\sigma$ )	1.7%	1.2%	0.8%	0.7%	0.5%

A Monte Carlo model, SAMCRT, was used to produce simulations that explicitly simulate surface conditions around Palmer Station. Inputs for the model are taken from daily meteorological observations at the station and images of surface conditions taken from the ground and from a tethered balloon in order to estimate surface reflectance. Aerosol optical depths shown in Figure 2 are retrieved from the MFRSR direct beam irradiances and independent estimates of the Rayleigh and ozone optical depths. These aerosol optical depths are used in model simulations which are then compared to the MFRSR measurements. The error bars represent an assumed error of 10% in the estimates of the total, Rayleigh, and ozone components.

Differences between the measurements and models for all three clear-sky days are presented in Table 2 for each wavelength and also integrated over the wavelength range of the MFRSR channels. Figures 3 and 4 show results for one of the observations days: January 17, 2000. Figure 3 represents the calibrated data as a difference between the measurements and modeled values for both total and diffuse irradiance. The discrepancy has strong wavelength dependence. Figure 4 represents the diffuse-to-total ratio

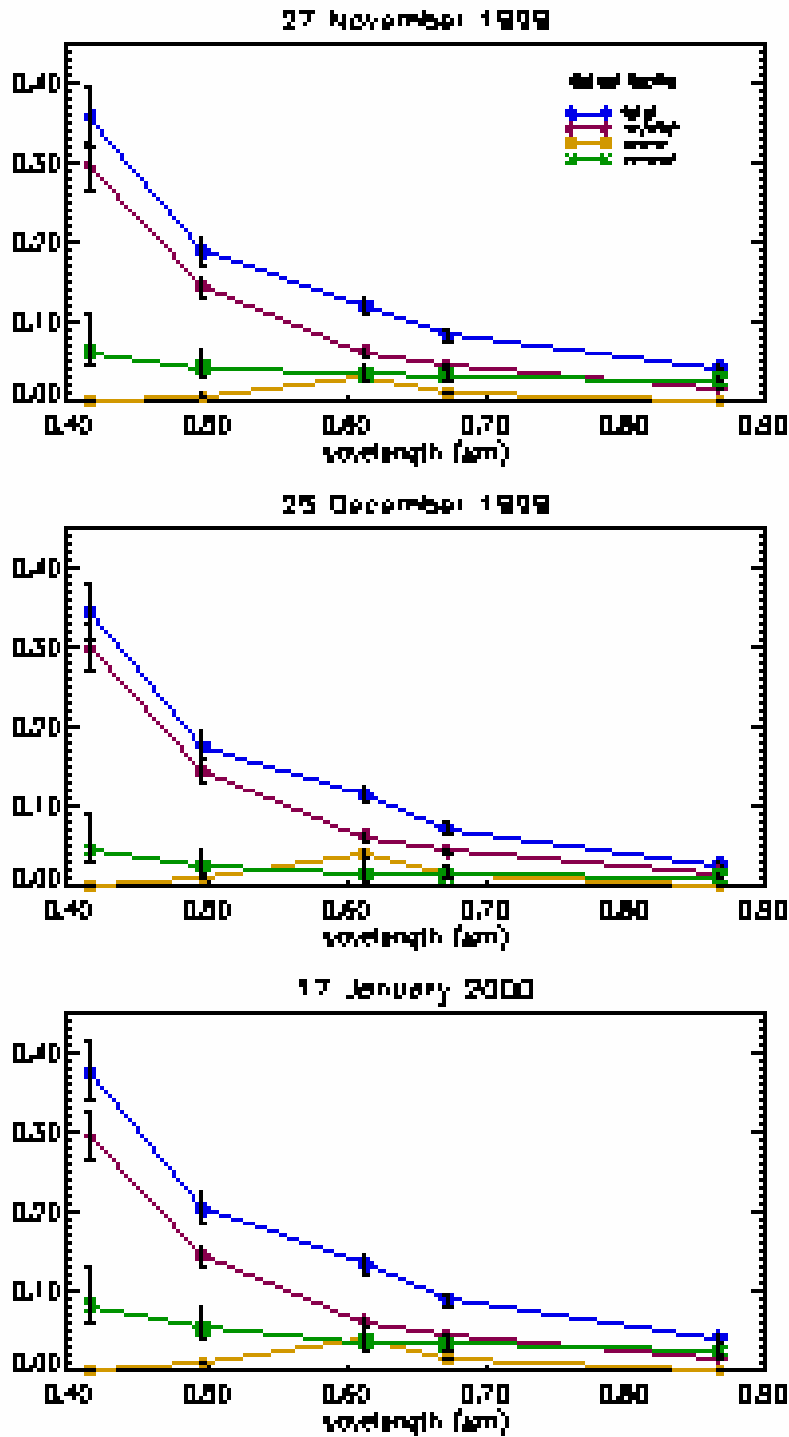


**Figure 2.** Total, Rayleigh, ozone, and aerosol optical depths for each day. Rayleigh optical depths are computed using measured surface pressure at the station and ozone concentrations are taken from TOMS.

**Table 2.** Average differences between measured and modeled values for total and diffuse irradiance for each of the clear-sky days in  $W\ m^{-2}\ \mu m^{-1}$ . The averages are for one hour around noon ( $n = 60$ ) except for November 27 when the average was made around 2:00pm due to a noon cloud passage. Values are integrated over the wavelength range of the 5 MFRSR channels and the percent of the total integrated diffuse value are given.

<b>November 27, 1999</b>				
<b>MFRSR Channel</b>	<b>Total</b>		<b>Diffuse</b>	
	<b>Measured</b>	<b>Difference</b>	<b>Measured</b>	<b>Difference</b>
<b>415 nm</b>	1066.1	31.6	312.8	-51.7
<b>500 nm</b>	1225.5	-12.0	205.5	-42.4
<b>615 nm</b>	1065.8	3.4	90.9	-24.5
<b>670 nm</b>	995.7	-1.3	66.2	-20.7
<b>870 nm</b>	632.3	9.9	27.2	-5.6
<b>Integrated <math>W\cdot m^{-2}</math></b>	448.6	1.3 (0.3%)	52.7	-11.7 (22%)

<b>December 25, 1999</b>				
<b>MFRSR Channel</b>	<b>Total</b>		<b>Diffuse</b>	
	<b>Measured</b>	<b>Difference</b>	<b>Measured</b>	<b>Difference</b>
<b>415 nm</b>	1235.0	22.6	348.2	-53.2
<b>500 nm</b>	1400.5	-16.7	224.6	-30.0
<b>615 nm</b>	1198.8	9.8	97.9	-2.5
<b>670 nm</b>	1125.2	3.1	72.1	-0.9
<b>870 nm</b>	713.2	13.1	30.1	8.5
<b>Integrated <math>W\cdot m^{-2}</math></b>	509.2	1.8 (0.4%)	57.8	-4.7 (8.1%)

<b>January 17, 2000</b>				
<b>MFRSR Channel</b>	<b>Total</b>		<b>Diffuse</b>	
	<b>Measured</b>	<b>Difference</b>	<b>Measured</b>	<b>Difference</b>
<b>415 nm</b>	1103.7	32.2	301.4	-84.6
<b>500 nm</b>	1266.9	-7.4	189.6	-74.9
<b>615 nm</b>	1094.3	13.5	75.8	-42.2
<b>670 nm</b>	1025.3	1.3	52.3	-37.2
<b>870 nm</b>	653.7	11.4	18.7	-12.7
<b>Integrated <math>W\cdot m^{-2}</math></b>	462.7	3.1 (0.7%)	46.8	-20.7 (44.2%)

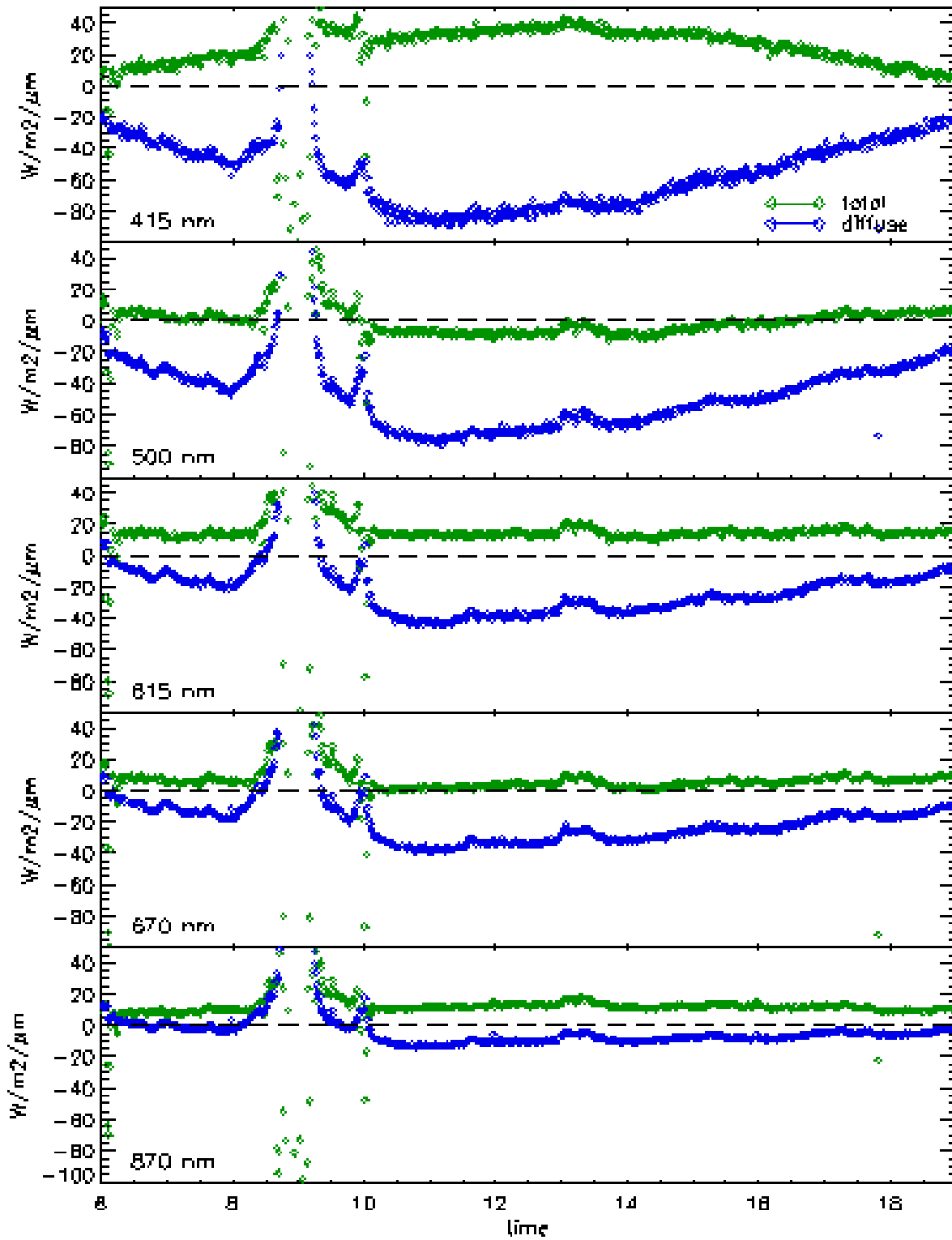
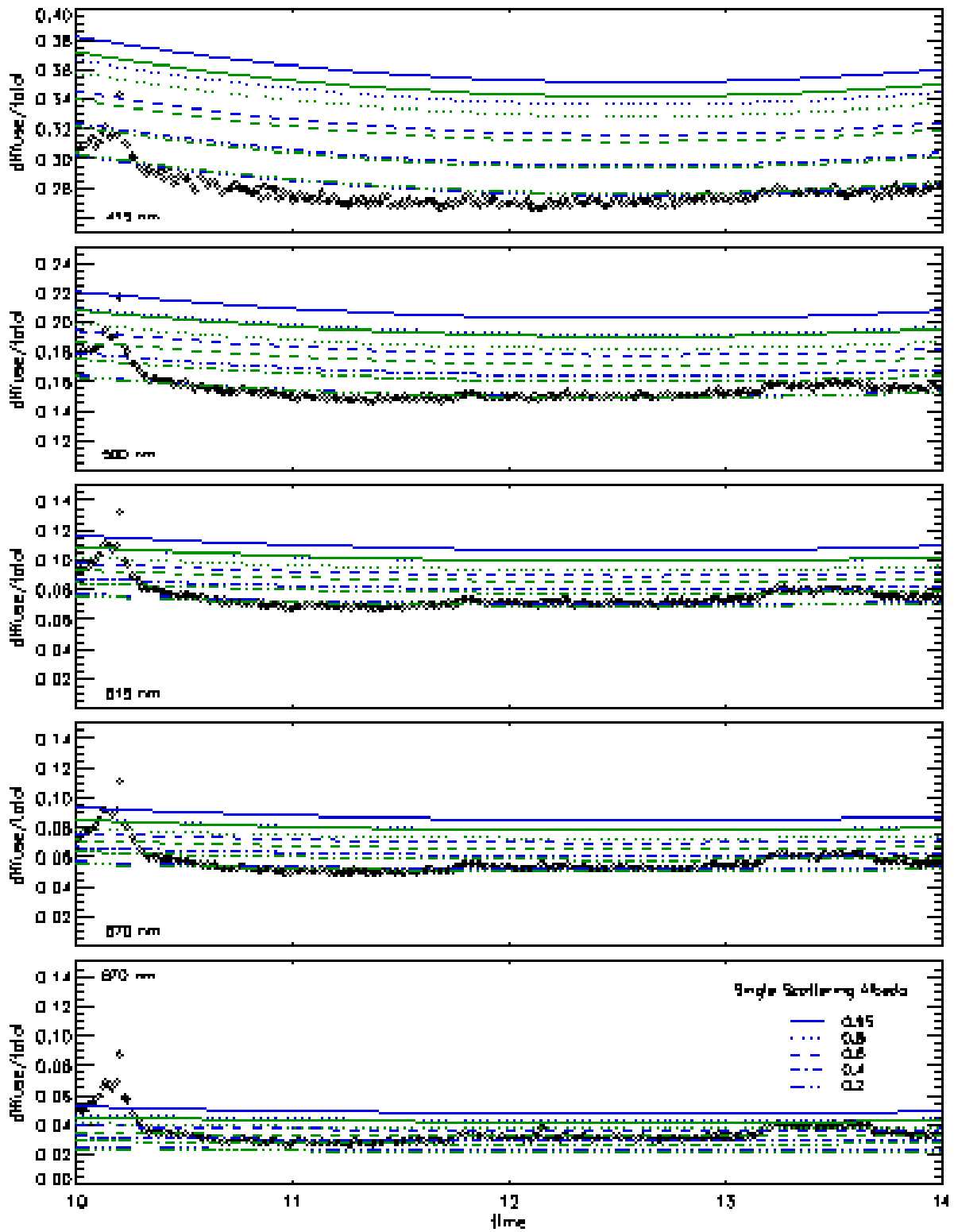


Figure 3. Measured minus modeled total (green) and diffuse (blue) irradiances for January 17, 2000.



**Figure 4.** Ratio of diffuse-to-total irradiances for January 17, 2000, for the MFRSR data (black symbols) and SAMCRT (lines) for different values of aerosol single scattering albedo.

(black symbols) for each channel to illustrate that the phenomenon is independent of instrument calibration. Sensitivity studies were performed in an attempt to reconcile the measurements and model results by modeling a molecular atmosphere and varying aerosol single scattering albedo (blue and green lines). Blue lines represent the MFRSR retrieved aerosol optical depths and green lines represent aerosol optical depths that biased low according to stated accuracy in the retrievals (Harrison et al. 1994). Decreasing the single scattering albedo of the aerosol does not reconcile the models to the data due to a mismatch in the spectral shape of the two.

## Conclusions

The diffuse anomaly is detected on each of the three clear-sky days that occurred during the Antarctic field season. The MFRSR measurements are within the 2% of the calibration error for a modeled molecular atmosphere. The anomaly exhibits strong wavelength dependence throughout the visible region and the magnitude of the anomaly is analogous to observations at other locations (ARM-CART). An aerosol single scattering albedo of 0.2 reconciles the measurements and models at shorter wavelengths but underestimates the measurements at longer wavelengths. Detection of the diffuse anomaly in the Antarctic suggests that an anthropogenic source may not be responsible for the absorption. Further examination of spectral data at various locations around the globe representing sites at different latitudes, altitudes, and proximity to urbanization may help to determine the process responsible for this discrepancy.

## Corresponding Author

Allison Payton, [Allison@icess.ucsb.edu](mailto:Allison@icess.ucsb.edu)

## References

Harrison, L., J. Michalsky, and J. Berndt, 1994: Automated multi-filter rotating shadow-band radiometer: An instrument for optical depth and radiation measurements. *Applied Optics*, **33**(22), 5118-5125.